European Journal of Pharmaceutical Sciences 176 (2022) 106249

Contents lists available at ScienceDirect

European Journal of Pharmaceutical Sciences

journal homepage: www.elsevier.com/locate/ejps

Peptide-based targeted cancer therapeutics: Design, synthesis and biological evaluation

Iwan Iwanov [a], Arianna Rossi [b,c], Monica Montesi [b], Irini Doytchinova [d,*], Armen Sargsyan [e], Georgi Momekov [d], Silvia Panseri [b,*], Emilia Naydenova [a,*]

[a] University of Chemical Technology and Metallurgy, 8 Blvd. Kliment Ohridski, Sofia 1756, Bulgaria
[b] Institute of Science and Technology for Ceramics, National Research Council of Italy, via Granarolo 64, Faenza (RA), Italy
[c] University of Messina, Department of Chemical, Biological, Pharmaceutical and Environmental Sciences, Piazza Pugliatti 1, Messina (ME), Italy
[d] Medical University of Sofia, 2 Dunav st., Sofia 1000, Bulgaria
[e] Scientific and Production Center "Armbiotechnology" NAS RA, 14 Gyurjyan str., Yerevan 0056, Armenia

ARTICLE INFO

Keywords:
Target therapy
Peptide drug design
Cancer
In vitro testing
Molecular docking

ABSTRACT

Cancer is the leading cause for human mortality together with cardiovascular diseases. Abl (Abelson) tyrosine kinases play a fundamental role in transducing various signals that control proliferation, survival, migration and invasion in several cancers such as Chronic Myeloid Leukemia (CML), breast cancer and brain cancer. For these reasons Abl tyrosine kinases are considered important biological targets in drug discovery. In this study a series of lysine-based oligopeptides with expected Abl inhibitory activity were designed resembling the binding of FDA-approved drugs (i.e. of Imatinib and Nilotinib), synthesized, purified by High Performance Liquid Chromatography (HPLC), analyzed by mass spectrometry (MS) and biologically tested *in vitro* in CML (AR-230 and K-562), breast cancers (MDA-MB 231 and MDA-MB 468) and glioblastoma cell lines (U87 and U118). The solid-phase peptide synthesis (SPPS) by Fmoc (9-fluorenylmethoxycarbonyl) chemistry was used to synthesize target compounds. AutoDock Vina was applied for simulation binding to Abl. The biological activities were measured evaluating cytotoxic effect, induction of apoptosis and inhibition of cancer cells migration. The new peptides exhibited different concentration-dependent antiproliferative effect against the tumor cell lines after 72 h treatment. The most promising results were obtained with the U87 glioblastoma cell line where a significant reduction of the migration ability was detected with one compound (H-Lys^1-Lys^2-Lys^3-NH_2).

1. Introduction

Cancer is the leading cause for human mortality together with cardiovascular diseases. Although conventional chemotherapy remains the principal cancer treatment, treating cancer with novel drugs will reduce the side effects providing better life and healthcare for many patients worldwide (Enbäck and Laakkonen, 2007).

New anticancer drugs with high metabolic stability and selectivity on the target should be discovered after identification of the most appropriate biological structures to be attacked: specific membrane receptors or enzymes (Enbäck and Laakkonen, 2007; Aina et al., 2002; Vlieghe et al., 2010).

The treatment against cancer includes the use of small molecule drugs as well as proteins, monoclonal antibodies and peptides (Vardanyan and Hruby, 2016). Small molecules, due to their advantages in efficacy and safety compared with traditional chemotherapy drugs in targeted cancer therapy, are emerging as cancer treatments (Zhong et al., 2021). The monoclonal antibodies (mAbs) and large protein ligands have two major limitations compared to peptides: (i) their large size leads to poor delivery to tumor issues; (ii) nonspecific uptake into the reticuloendothelial system causes dose-limiting toxicity to the liver and bone marrow (Qiu et al., 2007; Allen, 2002; Pastan et al., 2006; Reff et al., 2002; La Manna et al., 2021; La Manna et al., 2018).

The small peptides with anticancer activity containing specific amino acid sequences, are selective and toxic to cancer cells (Tyagi et al., 2015). They are a promising solution as therapeutic agents compared to antibodies and small molecules due to their high selectivity, high penetration and easy modifications (Thundimadathil, 2012; Vlieghe et al., 2010; Otvos, 2008). In addition, their degradation by proteolysis can be prevented by incorporation of D-amino acids or cyclization

* Corresponding authors.
E-mail addresses: idoytchinova@pharmfac.mu-sofia.bg (I. Doytchinova), silvia.panseri@istec.cnr.it (S. Panseri), emilia@uctm.edu (E. Naydenova).

https://doi.org/10.1016/j.ejps.2022.106249
Received 12 April 2022; Received in revised form 17 June 2022; Accepted 28 June 2022
Available online 30 June 2022

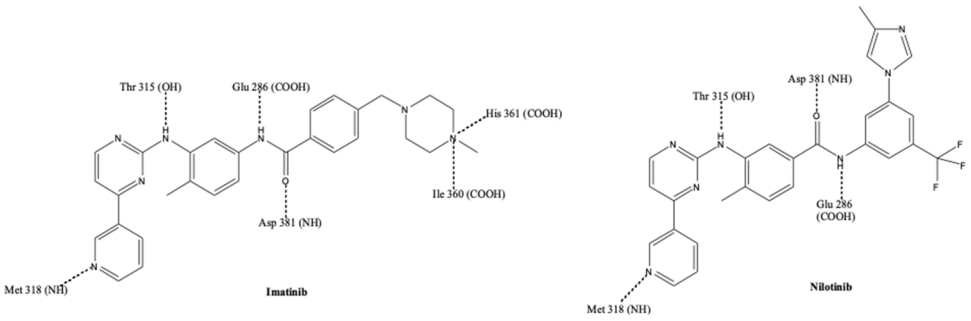

Fig. 1. H-binding of Imatinib and Nilotinib to Abl.

(Thayer, 2011; Borghouts et al., 2005). The direct use of peptides to treat cancer is raising more interest in the last years. In fact, their anticancer activity is the results of different mechanisms that limit tumor growth involving the inhibition of various biological processes (e.g. angiogenesis, protein-protein interactions, enzyme activity, signal transduction pathways, and cancer-related gene expression) (Rosca et al., 2011; Karagiannis and Popel, 2008; Kritzer et al., 2005; Mochly-Rosen and Qvit, 2010; Eldar-Finkelman and Eisenstein, 2009; Tonelli et al., 2005; Kakde et al., 2011; Zheng et al., 2011). Moreover anti-cancer peptides act as antagonists which can selectively bind specific receptors (Cornelio et al., 2007; Sotomayor et al., 2010), and induce apoptosis in tumor cells (Smolarczyk et al., 2006; Ellerby et al., 1999; Walensky et al., 2004; Hoskin and Ramamoorthy, 2008; Rodrigues et al., 2009; Droin et al., 2009).

Protein tyrosine kinases, are important regulators of several biological processes, and their abnormal activity has been identified as key factors in many human diseases, including cancer, diabetes, and neurodegenerative disorders (Blume-Jensen and Hunter, 2001; Cohen, 2002; Saltiel and Pessin, 2002; Neduva and Russell, 2006; Remenyi et al., 2005; Remenyi et al., 2006). For these reasons they are attractive targets for new drugs and peptides design. Among tyrosine kinases, in the last decades, it has been deeply investigated the Bcr-Abl-tyrosine kinase in Chronic Myeloid Leukemia (CML) (Hunter, 1997; Patarca, 1996; Al-Obeidi and Lam, 2000; Druker et al., 1996; Druker et al., 2001; Lam et al., 1995; Al-Obeidi et al., 1998; Goldman and Melo, 2001; Sawyers, 1999; Pophali and Mrinal, 2016; Deininger et al., 2000; Goldman, 2000). Four Bcr-Abl chains are gathered in close proximity, and it is easy for the kinase domains to attach phosphates to neighboring Bcr-Abl chains activating them. The result is the overexpressed protein production and the uncontrolled growth of the myeloid cells (Goodsell, 2005; Ganguly and Plattner, 2012; Wang and Pendergast, 2015).

Imatinib was the first Abl-tyrosine kinase inhibitor (STI571 - Gleevec, Novartis, Basel, Switzerland) approved by the Food and Drug Administration (FDA) in 2001, followed by other similar drugs such as Dasatinib, Nilotinib, Bosutinib and Ponatinib (LeMarbre et al., 2007; Aghel et al., 2017; Rossari et al., 2018). This drug's family works as competitive inhibitor of ATP's binding to Bcr-Abl-tyrosine kinase. These drugs interact with the enzyme when it is inactive, and the activation loop is closed and the peptide substrate cannot go in the active site and bind to C-lobe disturbing the first stage of protein synthesis catalysed by Bcr-Abl (Reddy and Aggarwal, 2012). In detail, Imatinib and Nilotinib prevent ATP from binding to Abl domain via six and four hydrogen interactions respectively (Fig. 1). Molecular dynamics simulations revealed the existence of intermediate state in Bcr-Abl between active and inactive form which is characterized by salt bridge between Glu-286 and Arg-386 (Reddy and Aggarwal, 2012).

Unfortunately, many patients develop resistance to these drugs. In addition these compounds inhibit also another tyrosine kinase receptor called c-KIT, which is found in bone marrow stem cells negatively affecting their division and differentiation, and prolonged treatment could alter the hematopoiesis and develop anemia as side effect (LeMarbre et al., 2007).

Table 1
ChemPLP scores of the designed peptides and the reference compounds.

Compound	Structure	ChemPLP
1	H-His-His-OH	60.9470
2	H-His-His-His-OH	72.3591
3	H-His-His-Lys-OH	78.0910
4	H-His-Lys-His-OH	69.9312
5	H-Lys-His-Lys-OH	78.7264
6	H-Lys-Lys-OH	64.8408
7	**H-Lys-Lys-Lys-OH**	**85.3253**
8	H-Lys-Lys-2-amino bicyclo[2.2.1]heptane-2-carboxylic acid	80.2276
9	H-Lys-Lys-His-OH	79.1934
10	Imatinib	94.9644
11	Nilotinib	108.0341
12	Bosutinib	90.4119
13	Ponatinib	112.6931
14	Bafetinib	110.2151

The development of new Abl inhibitors as potential drug candidates is the starting point of this work. By analyzing the structure-activity relationships and enzyme-inhibitor interactions, new peptide structures were design, synthesis and biological evaluated *in vitro* in six different cell lines of CML, breast cancer and glioblastoma.

2. Materials and methods

2.1. Peptide synthesis and characterization

The protected amino acids and Fmoc-Rink Amide 4-Methylbenzhydrylamine (MBHA) Resin were purchased from Iris Biotech (Germany). All other reagents and solvents were analytical or High Performance Liquid Chromatography (HPLC) grade and were bought from Merck (Germany). The Liquid chromatography–mass spectrometry (LC/MC) spectra were recorded on a Linear Ion Trap Mass Spectrometer (LTQ XL), Thermo Corporation, USA. The optical rotation was measured on automatic standard polarimeter Polamat A, Carl Zeis, Jena.

The conventional solid-phase peptide synthesis based on Fmoc (9-fluorenylmethoxycarbonyl) chemistry was employed to synthesize target compounds.

Rink-amide MBHA resin was used as a solid-phase carrier to obtain C- terminal amides. To prepare the peptides with C-terminal carboxyl group we used Wang resin. TBTU (2- (1H-benzotriazole-1-yl) -1,1,3,3-tetramethyluronium tetrafluoroborate) was used as a coupling reagent.

Three-functional amino acids were embedded as follows: Lys as Nα-Fmoc-Lys(Boc)-OH, Arg as Nα-Fmoc-Arg(Pbf)-OH. The coupling reactions were performed, using for amino acid/TBTU/1-Hydrozybenzotriazole (HOBt)/ N, N-Diisopropylethylamine (DIEA)/ resin a molar ratio 3/3/3/9/1 or amino acid/ N,N'-Diisopropylcarbodiimide (DIC)/HOBt/resin a molar ratio 3/3/3/1, respectively. The Fmoc-αNH-group was deprotected by treatment with 20% piperidine

solution in dimethylformamide.

The coupling and deprotection reactions were checked by the Kaiser test. The cleavage of the synthesized peptide from the resin was done, using a mixture of 95% trifluoroacetic acid (TFA), 2.5% triisopropylsilan (TIS) and 2.5 % water. The peptide was obtained as a filtrate in TFA and precipitated with cold dry ether. The precipitate was filtered, dissolved in water and lyophilized to obtain the crude peptide. The peptide purity was monitored on a RP-HPLC XTera C18 3.5 μm (125 × 2.1mm) (Waters Co.) column, flow 200 μl/min, using a linear binary gradient of phase B from 10% to 90% for 15 min (phase A: 0.1% HCOOH/H_2O; phase B: 0.1% HCOOH/ Acetonitrile) The compounds were checked by electrospray ionization mass spectrometry. The analytical data for the synthesized peptides is shown in Table 1.

2.2. Hydrolytic stability

Hydrolytic stability of targeted compounds was studied in a model system, which mimics pH values in the blood plasma. Model solution used for determination of hydrolytic stability was prepared according to the European Pharmacopoeia, 6th Edition, as follows: Buffer with pH 7.4 – 2.38 g Na_2HPO_4, 0.19 g KH_2PO_4 and 8.0 g NaCl was dissolved in dH2O. The obtained solution was made up to 1000.0 mL with dH2O. All analysis were monitored on Perkin-Elmer Series 200 HPLC with UV Detectors, column Hypersil GOLD C18 100 × 3 mm, 5 μm with isocratic mobile phase containing acetonitrile-water 35:65 (v/v), elution rate: 0.9 mL/min, room temperature, scanning wavelength 190 nm, injected volume 20 μL. Hydrolytic stability of all newly synthesized molecules was monitored for a period of 72 hours, and they all were completely stable in the test conditions.

2.3. Molecular docking

Protein preparation. The X-ray structure of wild-type Bcr-Abl (pdb code: 3OXZ) (Zhou et al., 2011) was retrieved from the Protein Data Bank (PDB). The hydrogen atoms were added and the water molecules were removed.

Dataset. The dataset consists of 9 novel peptidomimetic molecules designed to mimic the structure of Imatinib. They were built and molecular mechanics (MM) optimized (MM+ force field) applying steepest descent with root mean square (RMS) gradient of 0.1 kcal/(Amol) as implemented in HyperChem 8.0.6 (HyperChem 8.0.6, 2022). The structures of the reference compounds Imatinib, Nilotinib, Bosutinib, Ponatinib and Bafetinib were retrieved from DrugBank (Wishart et al., 2006, Jan 1) and MM optimized.

Molecular docking by GOLD. The X-ray structure of Bcr-Abl was used as a protein target in the docking simulations by GOLD v.5.2.2 software (GOLD Suite v5.2.2.2, 2022; Liebeschuetz et al., 2012). The docking of the novel and the reference compounds was performed at the following settings: ChemPLP scoring function, flexible ligand, rigid protein, radius of the binding site 6Å. ChemPLP incorporates protein-ligand interactions (attractive and repulsive contacts, hydrogen bonding, lipophilic interactions, acceptor-metal bonding) and clashes. Recent validation tests have shown it to be generally more effective than the other scoring functions for both pose prediction and virtual screening (Liebeschuetz et al., 2012). This scoring function is the default for GOLD version 5.1 and later. Each run generated 100 binding poses; the highest scored pose was selected for each molecule.

Molecular docking by AutoDock Vina. Studied chemical structures were built by ChemBioOffice 2010 (ChemBio3D Ultra12.0). Ligand free energy was minimized using MM2 force field and truncated Newton–Raphson method. Crystallographic structure of Bcr-Abl kinase was taken from the Protein Data Bank of Research Collaboratory for Structural Bioinformatics (PDB ID: 3OXZ). Inhibitor and water molecules were removed and polar hydrogens were added. Docking of ligand to enzyme has been done by using AutoGrid 4 and AutoDock Vina softwares (Trott and Olson, 2010; Russo et al., 2016). AutoDock Vina automatically calculates the grid maps and clusters the results in a way transparent to the user. The ligands were ranked using an energy-based scoring function and a grid-based protein-ligand interaction was used to speed up the score calculation. The most promising interaction models were chosen and for them hydrogen bounds lengths were measured.

2.4. Biological study

Cell culture. The antileukemic effects were evaluated in two chronic myeloid leukemia derived cell lines, namely AR-230 and K-562, expressing the fusion Bcr-Abl oncoprotein with tyrosine kinase activity (Koeffler and Golde, 1980; Wada et al., 1995). The cell lines used were grown as suspension cell cultures under standard conditions: RPMI - 1640 medium enriched with 10% fetal calf serum (FCS) and L-glutamine (2.5 mg/mL); humidified atmosphere with 5% carbon dioxide at 37°C (in an incubator). The leukemic lines were maintained in exponential growth phase by cell suspension removal and supplementation with fresh growth medium 2-3 times a week.

MDA-MB 231 and MDA-MB 468 Human Adenocarcinoma Cell Lines purchased from American Type Culture Collection (ATCC® HTB26™ and ATCC® HTB 132™, respectively) were culture in RPMI 1640 medium (Gibco) supplemented with 10% Foetal Bovine Serum (FBS) (Gibco) and 1% Penicillin-Streptomycin mixture (Pen/Strep) (Gibco, 100 U/ml -100 μg/mL). U87 Human Glioblastoma Cell line purchased from ATCC (ATCC® HTB-14™) were cultured in α-MEM nucleosides w/ o ascorbic acid medium (Gibco) added with 10% FBS and 1% Pen/Strep. U118 Human Glioblastoma Cell line purchased from ATCC (ATCC® HTB-15™) were cultured in DMEM High Glucose with pyruvate (Gibco) supplemented with 10% FBS and 1% Pen/Strep. Cell cultures were kept in an incubator at 37°C under controlled humidity and 5% CO_2 atmosphere conditions. Cells were detached from culture flasks by trypsinization and centrifugated. The cell number and viability were determined by Trypan Blue Dye Exclusion Test. All cell handling procedures were performed under a laminar flow hood in sterility conditions.

Peptide structures testing. A broad screening of E1, E2, E3, EN1, EN2 and EN3 on all cell lines was performed by testing various peptide's concentrations: 400 μM, 200 μM, 100 μM, 50 μM, 25 μM with AR-230 and K-56 cell lines; 300 μM, 200 μM, 100 μM, 50 μM, 25 μM, 10 μM, 5 μM, 1 μM and 0.5 μM with MDA-MB 231, MDA-MB 468, U87 and U118 cell lines. The peptides were resuspended firstly in MilliQ water and then diluted in cell culture (35x for 300 μM up to 5200x for 0.5 μM). Biological analyses on cells were performed 72 h after peptides' addition to the cell culture. Moreover, U87 cell line was subsequently selected for deeper analysis of cell apoptosis, migration and morphology after 72 h of exposure to EN1, EN2 and EN3 drugs at 100 μM concentration. Cells only were used as control group.

Cell viability Assay. The cellular viability of the leukemic cells was assessed by the MTT (3-(4,5-dimethylthiazol-2-yl)-2,5-diphenyltetrazolium bromide) reduction assay (Mosmann, 1983) with slight modifications (Konstantinov et al., 1999). In brief, exponentially proliferating cells were plated in 96- well flat-bottomed microplates (100 μl/well) at a density of 1.5 × 105 cells per ml and after 24h incubation at 37°C they were exposed to a range of concentrations of the tested compounds for 72 h. For each concentration a set of at 8 wells was used. After the treatment period 10 μl MTT solution (10 mg/ml in PBS - Phosphate-buffered saline) aliquots were added to each well and the microplates were further incubated for 4h at 37°C. Thereafter the MTT formazan crystals formed were dissolved through addition of 100 μl/well 5% formic acid solution in 2-propanol. The MTT-formazan absorption was measured using Beckman-Coulter DTX800 multimode microplate reader at 580 nm. Cell survival fractions were normalized as percentage of the solvent-treated control. In addition, IC50 values were derived from the concentration-response curves, using non-linear regression analysis (Curve fit, GraphPad Prizm software).

MDA-MB 231, MDA-MB 468, U118 and U87 cells were seeded 5.0 × 103 cells/well in 96 well-plates. Twenty-four hours after seeding, the

peptides were added to the cell cultures. Cell viability was performed by MTT assay after 72 h according to the manufacturer's instructions. Briefly, MTT reagent [3-(4,5-dimethylthiazol-2-yl)-2,5-diphenyltetrazolium bromide] (5 mg/mL) was dissolved in Phosphate Saline Buffer 1X (PBS 1X). At the time point, the cells were incubated with 10% media volume MTT solution for 2 h at 37°C, 5% CO2 and controlled humidity conditions. The media was removed and substituted with Dimethyl Sulfoxide (DMSO) (Merck) dissolving formazan crystals. After 15 min of incubation under slight stirring conditions, the absorbance of formazan was observed at 570 nm by using the Multiskan FC Microplate Photometer (Thermo Scientific). The values of absorbance are directly proportional to the number of metabolic active cells in each well. Two different experiments were performed and each sample was analyzed in triplicate (N=6).

ELISA assay. The hallmark for apoptosis DNA fragmentation pattern was examined using a commercially available 'Cell-death detection' ELISA kit (Roche Applied Science). This assay allows semi-quantitative determination of the histone-associated DNA-fragments. In brief, exponentially proliferating AR-230 cells were treated with equieffective concentrations of the tested agents and afterwards cytosolic fractions of 1 × 104 cells per group (treated or control) were utilized as antigen source in a sandwich ELISA with primary anti-histone antibody-coated microplate and a secondary peroxidase-conjugated anti-DNA antibody. The photometric immunoassay for determination of the histone-associated DNA fragments was carried out according to the manufacturers' instructions at 405 nm, using a Beckman-Coulter DTX800 multimode microplate reader. The results are expressed as oligonucleosomal enrichment factor (arbitrary unit representing a ratio between the absorption in the treated vs. the solvent-treated control samples).

Western blotting. 5.0 × 104 U87 cells per well were seeded in a 6 well-plate and exposed for 72 h to 100 μM concentration of EN1, EN2 and EN3 peptides. Cells only was used as a negative control. Briefly, cells were washed in PBS 1X and lysed in 100 μL/well Radioimmunoprecipitation Buffer (RIPA Buffer) supplemented with proteinase inhibitor cocktail (Cell Signaling). Protein concentration of each lysate supernatant was determined by a colorimetric assay (DC Protein Assay Kit, Bio-Rad), following the manufacturer's instructions. Equal amounts of total protein (20 μg) were loaded, separated at 200 V for ~ 45 min using 4−15% SDS-PAGE Stain-free protein gel (SDS PAGE Mini-PROTEAN TGX, Bio-Rad) and transferred by electrophoresis to a nitrocellulose membrane (Trans-Blot Turbo™, Bio-Rad). The membranes were washed in a solution of PBS 1X and 0.1% Tween 20, blocked with 2,5% skim milk for 40 min and incubated overnight at 4°C under soft agitation with primary antibodies: Pro-caspase 3 (Thermo Fisher Scientific MA1-41163, 2 μg/mL) and Actin (Invitrogen MA5-11869, 0.5 μg/mL) as the internal control. The membranes were washed and incubated with Goat Anti-Mouse IgG (H + L)-HRP Conjugate (Bio-Rad, 1:3000) for Pro-caspase 3 detection and with Goat Anti-Rabbit IgG (H + L)-HRP Conjugate (Bio-Rad, 1:3000) for Actin detection. One experiment with three biological replicates was performed. Bands were visualized by enhanced chemiluminescence (ChemiDOC XRS+, Bio-Rad) and analyzed with ImageLab software by applying Pro-caspase 3 bands normalization respect to Actin ones.

Apoptosis-DNA Ladder Kit. U87 cell line was seeded in T25 flasks (2.0 × 106) and exposed to 100 μM concentration of EN1, EN2 and EN3 peptides for 72 h. For apoptotic DNA evaluation, Apoptosis-DNA Ladder kit (Sigma) was performed following the manufacturer's instructions. Cells only group was used as negative control and U937 lyophilized apoptotic cells kit, provided by the manufacturer, was used as positive control. Briefly, total extract and purification of genomic DNA were performed and DNA was eluted in 100 μL Elution Buffer. The DNA of each sample was mixed with loading buffer (Merck) and then analysed by native agarose gel (1%) electrophoresis (1.5 h at 75 V voltage). The gel was visualized onto a UV light source and photograph by using the ChemiDOCX (Bio-Rad). One sample/group was analyzed.

Cell morphology evaluation. Morphology was evaluated by performing fluorescent analysis. In order to visualize actin filaments, cells (2.5×10^4 cells/well in 24 well-plate) exposed to 100 μM concentration of EN1, EN2 and EN3 drugs for 72 h were washed with PBS 1x for 5 min, fixed with 4% w/v paraformaldehyde (PFA) for 15 min and washed with PBS 1x for 5 min. Permeabilization was performed with PBS 1x with 0.1% (v/v) Triton X-100 for 5 min. F-actin filaments were highlighted with a red fluorescent solution of Rhodamine Phalloidin (Actin Red 555 Ready Probes™ Reagent, Invitrogen) for 30 min incubation at room temperature (Martin et al., 2017). Cells were washed with PBS 1x for 5 min and incubated with nuclear stain DAPI (4′,6-diamidino-2-phenylindole; Invitrogen) 300 nM in PBS 1x for 5 min. The nuclear morphological changes in apoptotic cells were also evaluated. Apoptotic cells were identified by condensation of chromatin and/or nuclear fragmentation (Lazebnik et al., 1993,Plotkin et al., 1999). The images were acquired by using an Inverted Ti-E Fluorescent Microscope (Nikon). One well/sample was performed (N=1).

Scratch Assay. The migration ability of U87 cell line was evaluated by performing the scratch assay during the 72 h exposure to 100 μM concentration of EN1, EN2 and EN3, by using cells only as a negative control (Liang et al., 2007). Cells were seeded 2.5×10^4 cells/well in 24 well-plate. After 24 h, the cell monolayer was scraped in a straight line to create a "scratch" with a p1000 pipet tip, then cells were washed by PBS 1X to remove cell debris, and cell culture medium containing drugs was added. A first image of the scratch was acquired at time 0, and then after 24, 48 and 72 h by an Inverted Ti-E Fluorescent Microscope (Nikon). For each image acquired, distances between one side of scratch and the other were measured and analyzed quantitatively by using ImageJ software. The results were graphically represented and statistically analyzed by using GraphPad Software (8.0.1 version). In addition, at each time points, cells were fixed with 4% w/v paraformaldehyde (PFA) and cell nuclei stained following the procedure described in "cell morphology evaluation" section, and the images were acquired by using an Inverted Ti-E Fluorescent Microscope (Nikon).

2.5. Statistical analysis

The results of MTT assay were elaborated by performing two-way analysis of variance (ANOVA) tests and were analyzed by using Dunnett's multiple comparisons test as a post-hoc test. Whereas a multiple T-test, Holm-Sidak method, with alpha = 0.05, was used to compare Scratch assay data. The results were expressed as mean ± standard error of the mean (SEM) plotted on the graph. Statistical analyses were performed by GraphPad Prism software (version 8.0.1, GraphPad Software, San Diego, CA, USA).

3. Results and discussion

The design of the new peptides with potential Abl inhibitory activity was based on structural units of Imatinib and Nilotinib, through which they interact with Bcr-Abl-tyrosine kinase. Imatinib and Nilotinib are competitive inhibitors of ATP for its binding site in Abl molecule. They form H-bonds with Met-318, Thr-315, Glu-286 and Asp-381. Imatinib makes two additional H-interactions with Ile-360 and His-361 (Weisberg et al., 2006; Weisberg et al., 2019; Savage and Antman, 2002). When a molecule of ATP goes into a specific binding pocket of Bcr-Abl the peptide substrate gets activated by the phosphorylation of one of its tyrosine residues interacting with other downstream effector molecules. When Imatinib occupies the place of ATP in the kinase pocket, the transfer of a phosphate group to the peptide substrate is getting impossible so no protein pro-duction catalyzed by Bcr-Abl will happen (Savage and Antman, 2002).

3.1. Molecular docking using GOLD Suite v5.2.2.2

In this study novel peptides were designed to act in a similar way of

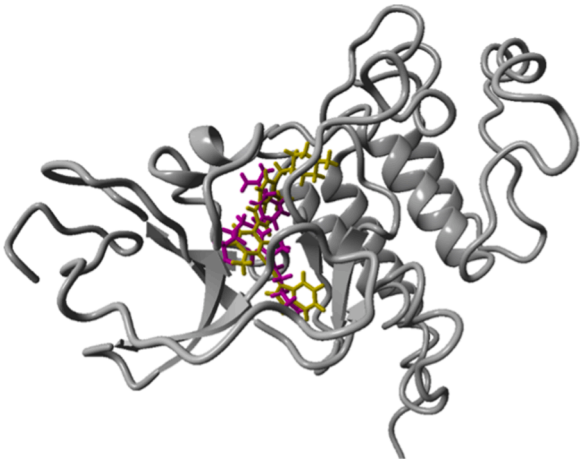

Fig. 2. Overlapped complexes Ponatinib (yellow)-Bcr-Abl (grey) and compound H-Lys-Lys-Lys-OH (magenta)-Bcr-Abl (grey).

Table 2
Binding free energy (ΔG) of the synthesized peptides.

Compound	Structure	Gibbs free energy (ΔG) kcal/mol
E1	H-Arg^1-Lys^2-Lys^3-Lys^4-OH	-6.9
E2	H-Phe^1-Phe^2-Lys^3-Arg^4-NH_2	-6.9
E3	H-Phe^1-Lys^2-Lys^3-Arg^4-NH_2	-6.7
EN1	H-Lys^1-Lys^2-Lys^3-Phe^4-OH	-7
EN2	H-Arg^1-Lys^2-Lys^3-Phe^4-OH	-7.1
EN3	H-Lys^1-Lys^2-Lys^3-NH_2	-7.3
7	H-Lys-Lys-Lys-OH	-6.7

Abl-tyrosine kinase inhibitors (i.e. Imatinib, Nilotinib, Bosutinib, Ponatinib, and Bafetinib), used as starting point for the molecular docking analysis.

The potential inhibitory activity of the peptides was performed by molecular docking using GOLD Suite v5.2.2.2. CCDC Software Ltd. Cambridge, UK. The X-ray coordinates of Bcr-Abl were used as a protein grid in the docking simulations by GOLD v.5.2.2 software (Zhou et al., 2011; HyperChem 8.0.6, 2022; Wishart et al., 2006, Jan 1; GOLD Suite v5.2.2.2, 2022). The ChemPLP scores of the docked compounds are given in Table 1 (the higher ChemPLP score corresponds to a better binding). The designed peptide structures showed lower ChemPLP scores than the reference compounds. The compound H-Lys-Lys-Lys-OH (compound 7 from the Table 1) showed the highest score

The overlapped structures of the complexes Ponatinib-Bcr-Abl and compound H-Lys-Lys-Lys-OH -Bcr-Abl showed that the inhibitors bind similarly in the binding site but compound H-Lys-Lys-Lys-OH (7) is shorter and makes fewer contacts with the enzyme than Ponatinib (Fig. 2). This could explain the lower ChemPLP score of this compound in comparison with Ponatinib.

We suppose that the expansion of the peptide structure will improve the binding affinity of the new inhibitors. That is why we chose the compound H-Lys-Lys-Lys-OH as the basic compound and designed a new series of lysine based tetrapeptides with expected biological activity.

3.2. Molecular docking by AutoDock Vina

On the base of preliminary docking simulations by GOLD v.5.2.2 software we selected H-Lys-Lys-Lys-OH as a leading compound and we designed and synthesized a new series of oligopeptides. Firstly, we have synthesized the compound that includes three lysine residues and that gives the highest ChemPLP scores. We decided to include the diamino acid lysine (Lys) in the designed peptides due to a similar spatial arrangement. The distance between the two nitrogen atoms bound to Thr-315 and Met-318 in the molecules of Imatinib and Nilotinib is 5

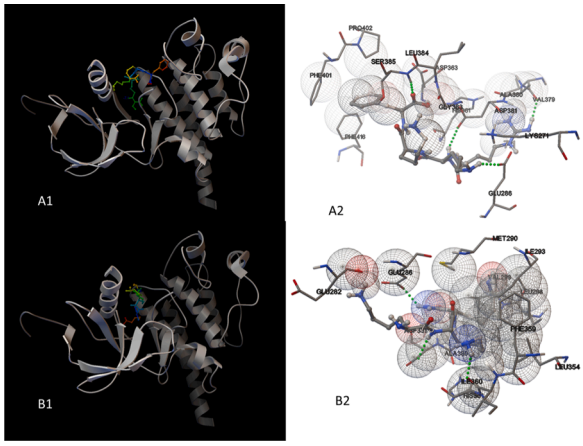

Fig. 3. Interaction of EN2 (A1, A2) and EN3 (B1, B2) with Bcr-Abl according to molecular docking analysis. In detail: A1 and A2, EN2 was found to form 4 hydrogen bonds with Bcr-Abl: phenylalanine carbonyl oxygen atom with amide NH of Ser-385 (2.088Å), side -NH2 group of first lysine (Lys at position 2) with side CO Glu-286 (2.065Å), NH from the peptide bond between Arg1 and Lys2 with carbonyl oxygen of Asp-381 (2.122Å) and NH of arginine with carbonyl oxygen of Val-379 (2.072Å). B1 and B2, in EN3 3 H-bonds were detected: one between amino group of C-terminal amide of EN3 and carbonyl oxygen atom of side chain of Glu-286 (2.093Å), second one between side amino group of Lys at position 2 of EN3 and carbonyl oxygen atom of Ile-360 (1.956Å), and the last one between second lysine peptide NH and CO Asp381 (2.098Å).

atoms (4 carbon and one nitrogen). Molecular docking binding to Bcr-Abl protein by using AutoGrid 4 and AutoDock Vina softwares were also performed. Results of molecular docking analysis are presented in the Table 2.

Based on the results from Table 2, EN2 and EN3 were identified as the most promising inhibitors of Bcr-Abl tyrosine kinase. For these compounds mode and type of interactions were inquired. The presence of two aromatic rings in the molecules of Imatinib and Nilotinib led us to include the amino acid phenylalanine (Phe) in the designed structures. The introduction of Phe at the N-terminus (E2 and E3) proved to be insignificant in contrast to its introduction at the C-terminus (EN1 and EN2) (Fig. 3 A1, A2)

The combination of Arg at position 1 and Phe at the C-terminus seems promising, because peptide EN2 forms 4 hydrogen bonds with the Bcr-Abl tyrosine kinase due to the presence of a guanidine residue that effectively interacts with carbonyl oxygen of Val-379 (2.072Å) from the Abl molecule (Fig 3A). In addition, arginine and lysine are basic amino acids and can easily form H-bonds with Glu-286. In case of EN3 (Fig. 3B) 3 H-bonds were detected: one between amino group of C-terminal amide of EN3 and carbonyl oxygen atom of side chain of Glu-286 (2.093Å), second one between side amino group of Lys at position 2 of EN3 and carbonyl oxygen atom of Ile-360 (1.956Å), and the last one between second lysine peptide NH and CO Asp381 (2.098Å).

The results showed that Arg-moiety of EN2 doesn't interact with Glu-286 as we have expected but with Val-379. The bond between amino group of C-terminal amide of EN3 and carbonyl oxygen atom of side chain of Glu-286 gives a confirmation that amide function is better than carboxylic group. The bonds between side -NH2 group of Lys at position 2 in EN2 with side CO Glu-286 and between side amino group of Lys at position 2 of EN3 and carbonyl oxygen atom of Ile-360 suggest that lysine should stay in the design element in further studies of new Abl inhibitors.

Compound EN3 was obtained as the C-terminal amide in order to prevent enzyme degradation. We expected that the amide function might interact more efficiently with the Bcr-Abl tyrosine kinase. This was confirmed by the better results in the study of biological activity (see below). The U87 cell line seems to be more affected by the presence of this peptide (Fig. 5). The introduction of highly hydrophilic Arg into

Table 3
Structures and characteristics of the synthesized peptides. Mm molecular mass; RT- retention time; *specific rotation [α] in water (c = 1).

Compound Name	Molecular Formula	Mm $_{exact}$	[MH] $^{+}$ Observed	RT (min)	(°)*
E1	$C_{24}H_{57}N_{10}O_8$	558.7252	558.4246	0.33	-32
E2	$C_{30}H_{50}N_8O_8$	595.7457	596.3720	0.73	-22
E3	$C_{27}H_{56}N_9O_8$	576.7433	577.3987	0.35	-6
EN1	$C_{27}H_{55}N_7O_9$	549.7142	550.3710	1.71	+30
EN2	$C_{27}H_{54}N_9O_8$	577.7276	578.3772	1.73	+18
EN3	$C_{18}H_{39}N_7O_3$	401.5533	402.3184	1.62	-6

Table 4
Cytotoxic effects of the tested compounds as assessed by the MTT-dye reduction assay after 72 h treatment.

Compounds	IC_{50} (μM) AR-230	K-562
E1	184.2	207.7
E2	157.2	135.0
E3	202.0	122.7
EN1	194.2	169.6
EN2	124.5	203.0
EN3	41.09	179.0
Imatinib	0.817	0.622

the N-terminus of lysine-based tetra peptide (E1) does not significantly affect biological activity. Molecular docking and simulation binding to Abl protein showed that this peptide formed only two Hydrogen bonds with Bcr-Abl tyrosine kinase (Fig. 1S Supplementary Materials). This could explain the low biological activity (Section 3.4).

Peptide EN2 reduces the cell viability by a higher percentage after 72 h of treatment of cells at concentrations above 50 μM. In comparison to Imatinib and Nilotinib which bind to NH-amide of Asp381 of Abl, the compounds EN1, EN2 and EN3 take part in H-interactions with carbonyl moiety of side chain of Asp381. E1, EN2 and EN3 bind to the carbonyl of side chain of Glu286 in the same way as Imatinib and Nilotinib. E2, E3 and EN3 bind to amide CO of Ile360 like Imatinib. H-bindings to Ser385, Glu282 and Val379 are made by some of studied peptides but are not described up to now in Imatinib and Nilotinib interactions.

The results show that the approach is correct, but the structures of the designed molecules need to be significantly optimized. The objective of ongoing docking is to look for relation between the found biological activity of the tested substances, and the results obtained from docking allow the design of new analogues with targeted biological activity.

3.3. Peptide synthesis

The compound 7 H-Lys-Lys-Lys-OH showed the highest score (ChemPLP 85.3253) close to Imatinib (ChemPLP 94.9644) (Table 1). This gave us the reason to design a new series of lysine-based peptides.

In order to study the effect of the amino acids Lys, Phe and Arg, we synthesized, purified and analyzed a series of new peptides.

The presence of each amino acid in the peptide design resembles building blocks of Imatinib and Nilotinib aiming to prevent a salt bridge formation in Abl intermediate states keeping the enzyme in its inactive form.

Phenylalanine is included in order to perform hydrophobic interactions with Abl.

Arginine is expected to bind to Glu-286 of Abl disturbing a salt bridge formation be-tween Glu-286 and Arg-386 in Abl structure.

The peptides were synthesized by standard solid phase peptide chemistry methods – Fmoc strategy. Some of the peptides (E2, E3, EN3) were synthesized as C-terminal amides in order to prevent enzyme degradation (Kim and Seong, 2001). The compounds were checked by LC-electrospray ionization mass spectrometry. The analytical data of synthesized peptides are reported in Table 3.

The hydrolytic stability of newly synthesized peptides was monitored for a period of 72 h in model buffer solution at pH values that mimic the pH in the blood plasma (pH 7.4) of the human body. They all were completely stable in the test conditions.

3.4. Biological studies

In order to verify the biological activity of the synthesized compounds, several cell lines were used. We started with CML cell lines (AR-230 and K-562) due to their well-known behavior when treated with tyrosine kinases inhibitors such as Imatinib, Nilotinib. Then we tested the new compounds also in solid tumor-derived cell lines (MDA-MB 231; MDA-MB 468; U87; U118). In fact, although several FDA-approved drugs targeting ABL kinases (e.g. Imatinib, Nilotinib) have been tested for the treatment of breast tumors and/or glioblastoma, their effectiveness is not well established due to the complexity of signaling pathways activated in solid tumors, the emergence of therapy resistance, and the fact these inhibitors have multiple cellular targets (Greuber

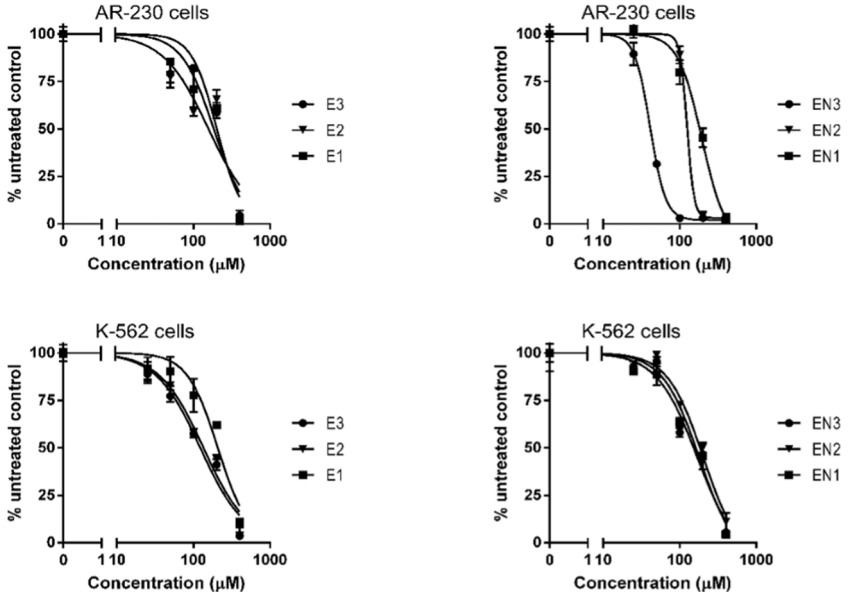

Fig. 4. Concentration-response inhibitory curves of the tested compounds as assessed by the MTT-dye reduction assay after 72 h treatment.

Table 5
Apoptotic DNA-fragmentation in AR-230 cells as assessed by Cell death detection ELISA™ kit.

Exposure	Enrichment factor		
	E2	E3	EN3
½ IC_{50} (for 24 h)	2.11 ± 0.24*	1.99 ± 0.20*	2.34 ± 0.31**
IC_{50} (for 24 h)	2.78 ± 0.17**	2.92 ± 0.25**	3.17 ± 0.14**

et al., 2013; Colicelli, 2010).

The synthetized peptides caused a concentration-dependent inhibition of the proliferation in the chronic myeloid leukemia derived cell lines AR-230 and K-562 after 72 h exposure. The concentration-response curves are presented in Fig. 4, and the IC50 values are summarized in Table 4. In AR-230 cells the most pronounced inhibitory activity is documented with EN3, EN2 and E2. In K-562, the lowest IC50 values were obtained for compounds E2 and E3. However the IC50 values are far from the Imatinib's value revealing a low biological activity in CML cell lines (Table 3; Fig. S2 in Supplementary Materials).

A mechanistic study to delineate the apoptogenic effects of the studied series showed that when administered at equieffective concentrations (fractions of IC50), compounds E2, E3 and EN3 caused an increase in the levels of histone-associated DNA fragments in the cytosole of treated AR-230 cells (Table 5). These data indicate that the inhibitory effects of the tested compounds against chronic myeloid leukemic cells are at least partly mediated by induction of apoptotic type programmed cell death.

Although it is well-known that ABL kinases are present also in solid tumors, less is known about their specific role. In addition, in contrast to the success of tyrosine kinases inhibitor therapies for the treatment of CML, the use of the ATP-competitive inhibitors such as imatinib, nilotinib and dasatinib has not achieved similar success for the treatment of solid tumors probably due to the heterogeneous nature of solid tumors, which often have acquired mutations in multiple tumor promoting pathways (Greuber et al., 2013; Colicelli, 2010). To verify if the new compounds could be more promising anti-cancer therapy in solid tumor respect CML, we tested the biological effect of the new peptide sequences in breast cancer and glioblastoma. In detail two breast cancer cell lines (MDA-MB 231 and MDA-MB 468) derived from triple-negative breast cancers (TNBC) characterized by poor prognosis compared to other subtypes due to their aggressive nature that lead to metastatic behavior, were employed (Wojtowicz et al., 2020). In addition two other cell lines (U118 and U87), derived from the most common malignant glioma in adults with high invasive nature and a high mortality rate were used in the biological studies (Zhang et al., 2016; DeAngelis, 2001). The responsiveness to Imatinib of these cells is known in literature, (Maher et al., 2001; Kadivar et al., 2018; Lo et al., 2011) and confirmed by our preliminary evaluation reported in Fig. S3 in Supplementary Materials.

An initial screening was performed in order to assess *in vitro* the cell cytotoxicity of the peptides. Cells, cultured in contact with different concentration of peptides (from 0.5 μM up to 300 μM), were analyzed after 72 h by MTT test, and the cell viability was compared to cells only used as control group. The low concentration of peptides (0.5 μM up to 25 μM) seems to not induce cytotoxicity to all the cell types tested (Fig. 5). Starting from 50 to 100 μM, we could appreciate a more pronounced dose-dependent cell viability reduction compared to cells only. In particular U87 cell line seems to be more affected by the presence of the peptides. In fact, the cell viability was reduced of ~ 40% after 72 h with EN1, EN2 and EN3 (Fig. 5D; 50 μM EN1 $p<0.05$, EN2 $p<0.01$, EN3 $p<0.001$; 100 μM EN1 $p<0.05$, EN2 $p<0.05$, EN3 $p<0.01$; 200 μM EN1 $p<0.05$, EN2 $p<0.05$, EN3 $p<0.01$; 300 μM EN1 $p<0.01$, EN2 $p<0.0001$). For these reasons we decided to use this cell line and these 3 peptides for further analysis, and 100 μM was chosen as reference concentration.

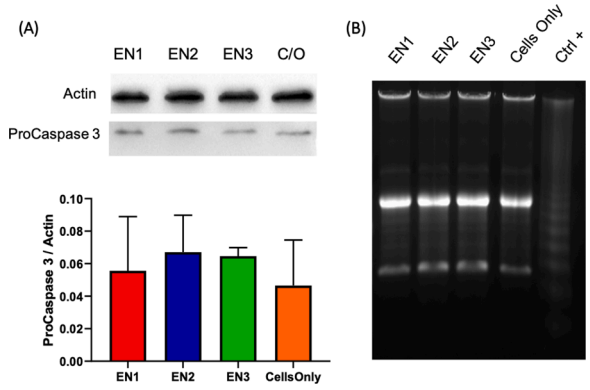

Fig. 6. (A) ProCaspase 3 protein expression measured by western blotting. The graph show the ProCaspase 3 level normalized to β-actin. B) DNA ladder pattern by agarose gel elettroforesis.

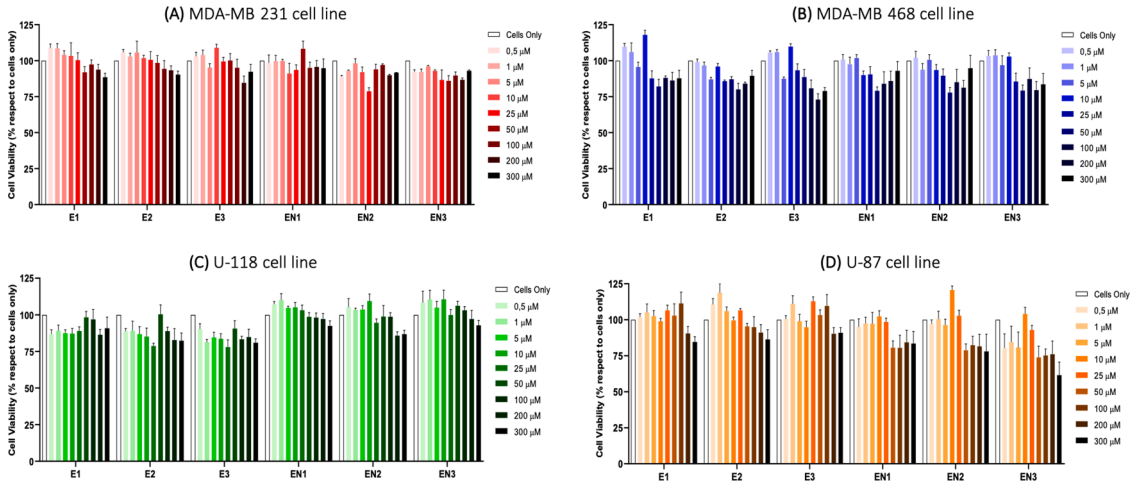

Fig. 5. Cell viability analysis. MTT assay was performed after 72 h of cell culture. The data show the percentage of viable cells compared to cells only as the control, and the mean ± standard error of the mean are presented. The graphs show the viability of MDA-MB 231 cell line (A), of MDA-MB 468 cell line (B), U118 cell line (C) and U87 cell line (D). In detail the following statistically significant differences were detected in U87 cell line comparing the compounds to cells only: 50 μM EN1 $p<0.05$, EN2 $p<0.01$, EN3 $p<0.001$; 100 μM EN1 $p<0.05$, EN2 $p<0.05$, EN3 $p<0.01$; 200 μM EN1 $p<0.05$, EN2 $p<0.05$, EN3 $p<0.01$; 300 μM EN1 $p<0.01$, EN2 $p<0.0001$.

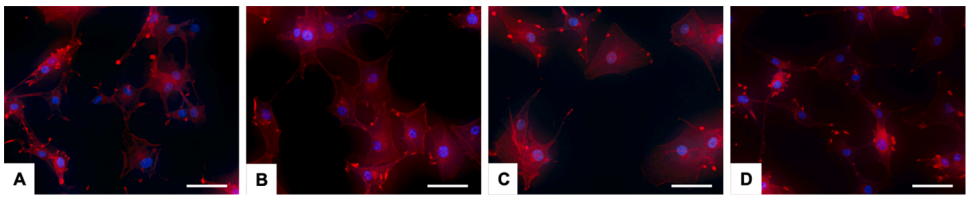

Fig. 7. Morphological analysis of U87 cell line cultured in the presence of 100 μM EN1 (B), EN2 (C), and EN3 (D) after 72 h. Cells only were used as control group (A). Phalloidin in red stains for actin filaments and DAPI in blue stains for cell nuclei. Scale bars: 50 μm.

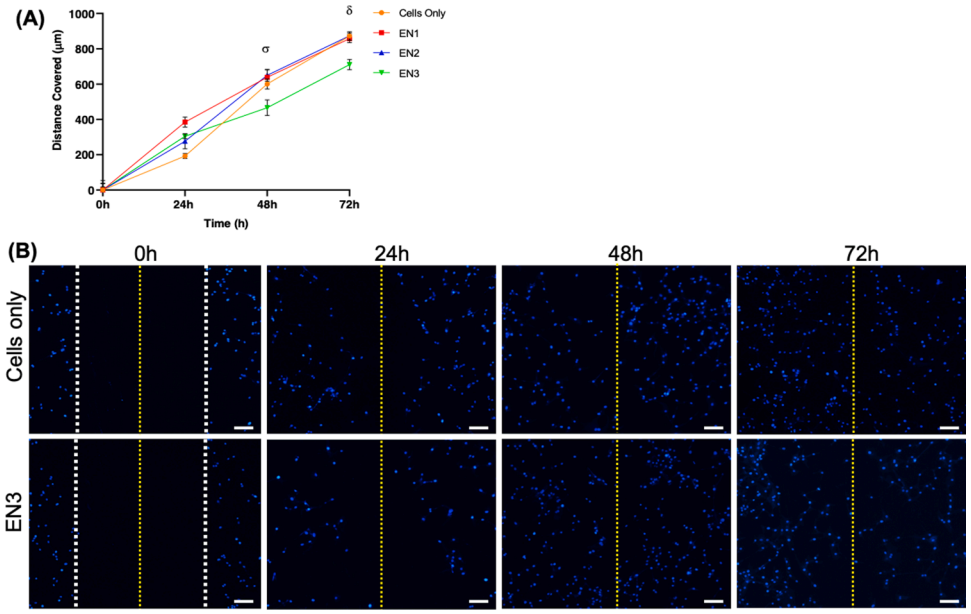

Fig. 8. In vitro scratch assay. (A) Quantitative analysis of scratch closure monitored over time. The scratch area was determined as the scratch area at a given time relative to the original area. Data are presented as the means ± SEM (N=3). EN3 is significantly different compared to the other groups and cells only at 48 and 72 h (σ: EN3 vs EN1 pvalue ≤ 0.01; EN3 vs EN2 p value ≤ 0.001; EN3 vs cells only pvalue≤0.05. δ EN3 vs all the other groups pvalue ≤ 0.01). (B) Representative images of the scratch assay. White dotted lined defined the distance between one side of scratch and the other (~ 650 μm). Yellow dotted line indicated the center of the scratch. Scale bars: 100 μm.

In order to check if the reduction in cell viability was triggered by apoptosis in response to specific damage induced by the peptides, we have analyzed by western blot the presence of Pro-Caspase 3 protein due to its central role in the execution-phase of cell apoptosis (Kamali et al., 2015; Chandra and Tang, 2009), by DNA ladder kit the presence of the DNA fragmentation, and by microscopic analysis of DAPI stained cells the nuclei morphology (Hengartner, 2000). The western blot results showed only the detection of the full-length of Pro Caspase 3 (Fig. 6A) with no statistically significantly difference among the peptides compared to cells only used as control group, indicating that the activation of the apoptosis process did not occurred. This was also confirmed by the DNA ladder kit that did not reveal any different pattern of DNA fragmentation compared to the cells only (Fig. 6B).

In accordance with these results, the DAPI staining analysis of cell nuclei, visualized by fluorescence microscope, showed the morphology of cell nuclei treated with the peptides was not different from the control group and did not exhibit chromatin, condensation and/or nuclear blebbing, typical apoptotic nuclear alteration (Fig. 7). A further analysis of actin filaments demonstrated typical cell morphology without aberrant differences among the group compared to cells only (Fig. 7).

These results demonstrated that the synthetized peptides did not trigger the apoptosis process and further investigation will be necessary to clarify the action mechanism. We assume that the detected activity of the compounds EN1, EN2, EN3 against U87 cells due to inhibition of Sarcoma (SCR) kinases, which are overexpressed in Glioblastoma (GBM) cells including U87, as it was found by Du et al. (Saadat et al., 2015).

An additional investigation was performed to better understand if the proposed peptides could have a key role in the inhibition of the cell migration/invasiveness. In fact, one of the clinical distinctive trait of glioblastoma is extensive infiltration of the tumor surrounding parenchyma, that almost never metastasize out of the brain (Du et al., 2009; Li et al., 2019). Invasion happens along pre-existing structures such as blood vessels, white matter tracts and the subarachnoid space, but the mechanisms leading to invasion of glioblastoma, and of tumors in general, are still not well understood (Vollmann-Zwerenz et al., 2020; Yelskaya et al., 2013). In vitro scratch assay was used as easy, low-cost and well-developed method to measure cell migration of U87 cell lines in contact with EN1, EN2 and EN3 peptide. This method is based on the observation that, upon creation of an artificial gap, so called “scratch”, on a confluent cell monolayer, the cells on the edge of the newly created gap will move toward the opening to close the “scratch” until new cell–cell contacts are established again (Liang et al., 2007). The cell cultures were analysed every 24 h for 3 days. In detail the dimension of the scratch was quantified by using ImageJ software and, starting from 48 h a significant reduction of the migration ability was detected in group EN3 compared to other groups EN1 (p value ≤ 0.01) and EN2 (p value ≤ 0.001) and the cells only (p value≤0.05). This statistical difference is maintained at 72 h for all the conditions (p value ≤ 0.01; Fig. 8A). A qualitative analysis was also performed and presented in Fig. 8B.

This result, if confirmed with further investigated, will represent the starting point for the optimization of the peptide sequence in order to obtain an anti-invasive treatment strategy in aggressive tumor such as glioblastoma.

4. Conclusions

Lysine-based oligopeptides has been designed and synthesized in order to act in similar way of the FDA-approved tyrosine kinase inhibitors. Biological studies performed on cancer cell lines with Abl over

expression revealed that the designed peptides possess moderate activity. The presence of Arg and Phe separately (in E1 and EN1) and together (in E2, E3 and EN2) is not enough for strong binding to Abl, so the design of the molecules should be optimized by the inclusion of other amino acids in search of new Abl inhibitors with anticancer activity. The best results, obtained with the cell line U87, represent the starting point for future optimization of the peptide sequence in order to obtain an anti-invasive treatment therapy in aggressive solid tumor such as glioblastoma.

Funding

This research was funded by Ministry of Education and Science (Republic of Bulgaria), National Program "EUROPEAN SCIENTIFIC NETWORKS", project "Drug molecule", grant number D01-278/05.10.2020.

Supplementary materials

Supplementary materials are available online and they contain the interaction of compounds E1, E2, E3 and EN1 with Bcr-Abl according to molecular docking analysis using AutoDock Vina softwares. A graph showing MTT positive control performed using Imatinib at the same peptide concentrations tested on MDA-MB 231, MDA-MB 468 and U118, U87.

CRediT authorship contribution statement

Iwan Iwanov: Conceptualization, Methodology, Investigation, Writing – original draft. **Arianna Rossi:** Methodology, Investigation, Writing – original draft. **Monica Montesi:** Conceptualization, Methodology, Validation, Investigation, Writing – original draft, Writing – review & editing. **Irini Doytchinova:** Writing – original draft. **Armen Sargsyan:** Methodology, Investigation. **Georgi Momekov:** Methodology, Writing – original draft. **Silvia Panseri:** Conceptualization, Methodology, Validation, Investigation, Writing – original draft, Writing – review & editing, Funding acquisition. **Emilia Naydenova:** Methodology, Investigation, Writing – original draft, Writing – review & editing, Funding acquisition.

Declaration of Competing Interest

The authors declare no conflict of interest.

Acknowledgments

The authors acknowledge E. Giusto and G. Bassi from Institute of Science and Technology for Ceramics, National Research Council of Italy for technical support in biological analysis.

Supplementary materials

Supplementary material associated with this article can be found, in the online version, at doi:10.1016/j.ejps.2022.106249.

References

Aghel, N., Delgado, D.H., Lipton, J.H., 2017. Cardiovascular toxicities of BCR-ABL tyrosine kinase inhibitors in chronic myeloid leukemia: preventive strategies and cardiovascular surveillance. Vasc Health Risk Manag. 13, 293–303.
Aina, O.H., Sroka, T.C., Chen, M.L., Lam, K.S., 2002. Therapeutic cancer targeting peptides. Biopolymers 66 (3), 184–199.
Al-Obeidi, F.A., Lam, K.S., 2000. Development of inhibitors for protein tyrosine kinases. Oncogene 19 (49), 5690–5701.
Al-Obeidi, F.A., Wu, J.J., Lam, K.S., 1998. Protein tyrosine kinases: structure, substrate specificity, and drug discovery. Pept. Sci. 47 (3), 197–223.
Allen, T.M., 2002. Ligand-targeted therapeutics in anticancer therapy. Nat. Rev. Cancer 2, 750–763.
Blume-Jensen, P., Hunter, T., 2001. Oncogenic kinase signalling. Nature 411 (6835), 355–365.
Borghouts, C., Kunz, C., Groner, B., 2005. Current strategies for the development of peptide-based anti-cancer therapeutics. J. Pept. Sci. 11 (11), 713–726.
Chandra, D.; Tang, D.G. Detection of apoptosis in cell-free systems. In: *Apoptosis*, Erhardt, P., Toth A., Eds Humana Press, Totowa, NJ, 2009, 559, 65-75.
Cohen, P., 2002. Protein kinases-the major drug targets of the twenty-first century? Nat. Rev. Drug Discov 1 (4), 309–315.
Colicelli, J., 2010 Sep 14. ABL tyrosine kinases: evolution of function, regulation, and specificity. Sci. Signal. 3 (139), re6.
Cornelio, D.B., Roesler, R., Schwartsmann, G., 2007. Gastrin-releasing peptide receptor as a molecular target in experimental anticancer therapy. Ann. Oncol. 18 (9), 1457–1466.
DeAngelis, L.M., 2001. Brain tumors. N. Engl. J. Med. 344, 114–123.
Deininger, M.W.N., Goldman, J.M., Melo, J.V., 2000. The molecular biology of chronic myeloid leukemia. Blood 96 (10), 3343–3356.
Droin, N., Hendra, J.B., Ducoroy, P., Solary, E., 2009. Human defensins as cancer biomarkers and antitumour molecules. J. Proteomics 72, 918–927.
Druker, B.J., Tamura, S., Buchdunger, E., Ohno, S., Segal, G.M., Fanning, S., Zimmermann, J., Lydon, N.B., 1996. Effects of a selective inhibitor of the Abl tyrosine kinase on the growth of Bcr–Abl positive cells. Nat. Med. 2 (5), 561–566.
Druker, B.J., Talpaz, M., Resta, D.J., Peng, B., Buchdunger, E., Ford, J.M., Lydon, N.B., Kantarjian, H., Capdeville, R., Ohno-Jones, S., Sawyers, C.L., 2001. Efficacy and safety of a specific inhibitor of the BCR-ABL tyrosine kinase in chronic myeloid leukemia. N. Engl. J. Med. 344 (14), 1031–1037.
Du, J., Bernasconi, P., Clauser, K.R., Mani, D.R., Finn, S.P., Beroukhim, R.;., Burns, M., Julian, B.;., Peng, X.P., Hieronymus, H., Maglathlin, R.L., Lewis, T.A., Liau, L.M., Nghiemphu, P.;., Mellinghoff, I.K., Louis, D.N., Loda, M., Carr, S.A., Kung, A.L., Golub, T.R., 2009. Bead-based profiling of tyrosine kinase phosphorylation identifies SRC as a potential target for glioblastoma therapy. Nat. Biotechnol. 27 (1), 77–83.
Eldar-Finkelman, H., Eisenstein, M., 2009. Peptide inhibitors targeting protein kinases. Curr. Pharm. Des. 15 (21), 2463–2470.
Ellerby, H.M., Arap, W., Ellerby, L.M., et al., 1999. Anti-cancer activity of targeted pro-apoptotic peptides. Nat. Med. 5 (9), 1032–1038.
Enbäck, J., Laakkonen, P., 2007. Tumour-homing peptides: tools for targeting, imaging and destruction. Biochem. Soc. Trans 35 (4), 780–783.
Ganguly, S.S., Plattner, R., 2012. Activation of Abl family kinases in solid tumors. Genes Cancer 3 (5-6), 414–425.
GOLD Suite v5.2.2.2, 2022. CCDC Software Ltd, Cambridge, UK.
Goldman, J.M., Melo, J.V., 2001. Targeting the BCR-ABL tyrosine kinase in chronic myeloid leukemia. N. Engl. J. Med. 344 (14), 1084–1086.
Goldman, J.M., 2000. Tyrosine-kinase inhibition in treatment of chronic myeloid leukaemia. Lancet 355, 1031–1032.
Goodsell, D.S., 2005. The Onkologist 10 (9), 758–759.
Greuber, E.K, Smith-Pearson, P., Wang, J., Pendergast, A.M., 2013 Aug; 13. Role of ABL family kinases in cancer: from leukemia to solid tumors. Nat. Rev. Cancer (8), 559–571.
Hengartner, M., 2000. The biochemistry of apoptosis. Nature 407, 770–776.
Hoskin, D.W., Ramamoorthy, A., 2008. Studies on anticancer activities of antimicrobial peptides. Biochim. Biophys. Acta 1778, 357–375.
Hunter, T., 1997. Oncoprotein networks. CellCell 88 (3), 333–346.
HyperChem 8.0.6, 2022. HyperCube, Inc.
Kadivar, A., Ibrahim Noordin, M., Aditya, A., Kamalidehghan, B., Davoudi, E.T., Sedghi, R., Akbari Javar, H., 2018. Antiproliferative effects of imatinib mesylate on ZR751 and MDAMB231 cell lines via PDGFRβ, PDGFBB, cKit and SCF expression. Int. J. Mol. Med. 42 (1), 414–424.
Kakde, D., Jain, D., Shrivastava, V., Kakde, R., Patil, A.T., 2011. Cancer therapeutics-opportunities, challenges and advances in drug delivery. J. Appl. Pharm. Sci 1 (9), 1–10.
Kamali, M., Dinarvand, R., Maleki, H., Arzani, H., Mahdaviani, P., Nekounam, H., Adabi, M., Khosravani, M., 2015. Preparation of imatinib base loaded human serum albumin for application in the treatment of glioblastoma. RSC Adv. 5, 62214–62219.
Karagiannis, E.D., Popel, A.S., 2008. Novel anti-angiogenic peptides derived from ELR-containing CXC chemokines. J. Cell. Biochem. 104 (4), 1356–1363.
Kim, K.H., Seong, B.L., 2001. Peptide Amidation: Production of Peptide Hormones in vivo and in vitro. Biotechnol. Bioprocess Eng. 6 (4), 244–251.
Koeffler, H.P., Golde, D.W., 1980. Human myeloid leukemia cell lines: a review. Blood 56 (3), 344–350.
Konstantinov, S.M., Eibl, H., Berger, M.R., 1999. BCR-ABL influences the antileukaemic efficacy of alkylphosphocholines. Br. J. Haematol. 107 (2), 365–374.
Kritzer, J.A., Stephens, O.M., Guarracino, D.A., Reznika, S.K., Schepartza, A., 2005. β-Peptides as inhibitors of protein-protein interactions. Bioorg. Med. Chem. 13, 11–16.
La Manna, S., Di Natale, C., Florio, D., Marasco, D, 2018. Peptides as therapeutic agents for inflammatory-related diseases. Int. J. Mol. Sci. 19 (9), 2714.
La Manna, S., Lopez-Sanz, L., Bernal, S., Fortuna, S., Mercurio, F.A., Leone, M., Gomez-Guerrero, C., Marasco, D, 2021. Cyclic mimetics of kinase-inhibitory region of Suppressors of Cytokine Signaling 1: progress toward novel anti-inflammatory therapeutics. Eur. J. Med. Chem. 221, 113547.
Lam, K.S., Wu, J., Lou, Q., 1995. Identification and characterization of a novel synthetic peptide substrate specific for Src-family protein tyrosine kinases. Int. J. Pept. Protein Res. 45 (6), 587–592.
Lazebnik, Y.A., Cole, S., Cooke, C.A., Nelson, W.G., Earnshaw, W.C., 1993. Nuclear events of apoptosis in vitro in cell-free mitotic extracts: a model system for analysis of the active phase of apoptosis. J. Cell Biol. 123 (1), 7–22.

LeMarbre, G., Schinstock, C., Hoyer, R., Krook, J., Tefferi, A., 2007. Late onset aplastic anemia during treatment of chronic myeloid leukemia with imatinib mesylate. Leuk. Res. 31 (3), 414–415.
Li, C., Wang, S., Yan, J.L., Torheim, T., Boonzaier, N.R., Sinha, R., Matys, T., Markowetz, F., Price, S.J., 2019. Characterizing tumor invasiveness of glioblastoma using multiparametric magnetic resonance imaging. J. Neurosurg. 132 (5), 1465–1472.
Liang, C.C., Park, A.Y., Guan, J.L., 2007. In vitro scratch assay: a convenient and inexpensive method for analysis of cell migration in vitro. Nat. Protoc. 2, 329–333.
Liebeschuetz, JW, Cole, JC, Korb, O., 2012. Pose prediction and virtual screening performance of GOLD scoring functions in a standardized test. J. Comput. Aided Mol. Des. 26 (6), 737–748.
Lo, Y.H., Ho, P.C., Zhao, H., Wang, S.C., 2011. Inhibition of c-ABL sensitizes breast cancer cells to the dual ErbB receptor tyrosine kinase inhibitor lapatinib (GW572016). Anticancer Res. 31 (3), 789–795.
Maher, E.A., Furnari, F.B., Bachoo, R.M., Rowitch, D.H., Louis, D.N., Cavenee, W.K., DePinho, R.A., 2001. Malignant glioma: genetics and biology of a grave matter. Genes Dev. 15 (11), 1311–1333.
Martin, J.L., Mendonça, L.M., Angert, I., Mueller, J.D., Zhang, W., Mansky, L.M., 2017. Disparate contributions of human retrovirus capsid subdomains to Gag-Gag oligomerization, virus morphology, and particle biogenesis. J. Virol. 91 (14), e00217–e00298.
Mochly-Rosen, D., Qvit, N., 2010. Peptide inhibitors of protein-protein interactions: from rational design to the clinic. Chim. Oggi – Chem. Today 28 (1), 14–16.
Mosmann, T., 1983. Rapid colorimetric assay for cellular growth and survival: application to proliferation and cytotoxicity assays. J. Immunol. Methods 65, 55–63.
Neduva, V., Russell, R.B., 2006. Peptides mediating interaction networks: new leads at last. Curr. Opin. Biotechnol 17 (5), 465–471.
Otvos Jr., L., 2008. Peptide-based drug design: here and now. Methods Mol. Biol. 494, 1–8.
Pastan, I., Hassan, R., Fitzgerald, D.J., Kreitman, R.J., 2006. Immunotoxin therapy of cancer. Nat. Rev. Cancer 6, 559–565.
Patarca, R., 1996. Protein phosphorylation and dephosphorylation in physiologic and oncologic processes. Crit. Rev. Oncog. 7, 343–432.
Plotkin, L.I., Weinstein, R.S., Parfitt, A.M., Roberson, P.K., Manolagas, S.C., Bellido, T., 1999. Prevention of osteocyte and osteo-blast apoptosis by bisphosphonates and calcitonin. J. Clin. Investig. 104 (10), 1363–1374.
Pophali, P.A., Mrinal, M.P., 2016. The role of new tyrosine kinase inhibitors in chronic myeloid leukemia. Cancer J. 22 (1), 40–50.
Qiu, X.Q., Wang, H., Cai, B., Wang, L.L., Yue, S.T., 2007. Small antibody mimetics comprising two complementarity-determining regions and a framework region for tumor targeting. Nat. Biotechnol. 25 (8), 921–929.
Reddy, E.P., Aggarwal, A.K., 2012. The Ins and Outs of Bcr-Abl inhibition. Genes Cancer 3 (5-6), 447–454.
Reff, M.E., Hariharan, K., Braslawsky, G., 2002. Future of monoclonal antibodies in the treatment of hematologic malignancies. Cancer Control 9 (2), 152–166.
Remenyi, A., Good, M.C., Bhattacharyya, R.P., Lim, W.A., 2005. The role of docking interactions in mediating signaling input, output, and discrimination in the yeast MAPK network. Mol. Cell 20 (6), 951–962.
Remenyi, A., Good, M.C., Lim, W.A., 2006. Docking interactions in protein kinase and phosphatase networks. Curr. Opin. Struct. Biol 16 (6), 676–685.
Rodrigues, E.G., Dobroff, A.S., Taborda, C.P., Travassos, L.R., 2009. Antifungal and antitumor models of bioactive protective peptides. An. Acad. Bras. Cienc. 81, 503–520.
Rosca, E.V., Koskimaki, J.E., Rivera, C.G., Pandey, N.B., Tamiz, A.P., Popel, A.S., 2011. Anti-angiogenic peptides for cancer therapeutics. Curr. Pharm. Biotechnol. 12 (8), 1101–1116.
Rossari, F., Minutolo, F., Orciuolo, E., 2018. Past, present, and future of Bcr-Abl inhibitors: from chemical development to clini-cal efficacy. J. Hematol. Oncol. 11, 1–14.
Russo, A., Scognamiglio, P.L., Hong Enriquez, R.P., Santambrogio, C., Grandori, R., Marasco, D., Giordano, A., Scoles, G., Fortuna, S., 2016. In silico generation of peptides by replica exchange Monte Carlo: docking-based optimization of Maltose-binding-protein ligands. PLoS One 11 (10), e0165349.
Saadat, Y.R., Saeidi, N., Vahed, S.Z., Barzegari, A., Barar, J., 2015. An update to DNA ladder assay for apoptosis detection. Bioimpacts 5 (1), 25–28.
Saltiel, A.R., Pessin, J.E., 2002. Insulin signaling pathways in time and space. Trends Cell Biol. 12 (2), 65–71.
Savage, D.G., Antman, K.H., 2002. Imatinib mesylate—a new oral targeted therapy. N. Engl. J. Med. 346 (9), 683–693.
Sawyers, C.L., 1999. Chronic myeloid leukemia. N. Engl. J. Med. 340, 1330–1340.
Smolarczyk, R., Cichoń, T., Graja, K., Hucz, J., Sochanik, A., Szala, S., 2006. Antitumor effect of RGD-4C-GG-D(KLAKLAK)2 peptide in mouse B16(F10) melanoma model. Acta Biochim. Pol. 53 (4), 801–805.
Sotomayor, S., Muñoz-Moreno, L., Carmena, M.J., et al., 2010. Regulation of HER expression and transactivation in human prostate cancer cells by a targeted cytotoxic bombesin analog (AN-215) and a bombesin antagonist (RC-3095). Int. J. Cancer 127 (8), 1813–1822.
Thayer, A.M., 2011. Improving peptides. Chem. Eng. News. 89, 13–20.
Thundimadathil, J., 2012. Cancer treatment using peptides: current therapies and future prospects. J. Amino Acids 2012, 967347.
Tonelli, R., Purgato, S., Camerin, C., et al., 2005. Antigene peptide nucleic acid specifically inhibits MYCN expression in human neuroblastoma cells leading to cell growth inhibition and apoptosis. Mol. Cancer Ther. 4 (5), 779–786.
Trott, O., Olson, A.J., 2010. Software News and Update AutoDock Vina: Improving the speed and accuracy of docking with a new scoring function, efficient optimization, and multithreading. J. Comput. Chem. 31, 455–461.
Tyagi, A., Tuknait, A., Anand, P., Gupta, S., Sharma, M., Mathur, D., Joshi, A., Singh, S., Gautam, A., Raghava, G.P., 2015. CancerPPD: a database of anticancer peptides and proteins. Nucleic Acids Res. 43, 837–843.
Vardanyan, R., Hruby, V., 2016. Synthesis of Best-Seller Drugs, 125. Academic Press, UK, pp. 495–534. London Wall, London EC2Y 5 AS.
Vlieghe, P;, Lisowski, V;, Martinez, J;, Khrestchatisky, M., 2010. Synthetic therapeutic peptides: science and market. Drug Discov. Today 15 (1-2), 40–56.
Vlieghe, P., Lisowski, V., Martinez, J., Khrestchatisky, M., 2010. Synthetic therapeutic peptides: science and market. Drug Discov. Today 15, 40–56.
Vollmann-Zwerenz, A., Leidgens, V., Feliciello, G., Klein, C.A., Hau, P., 2020. Tumor Cell Invasion in Glioblastoma. Int. J. Mol. Sci. 21 (6), 1932.
Wada, H., Mizutani, S., Nishimura, J., Usuki, Y., Kohsaki, M., Komai, M., Kaneko, H., Sakamoto, S., Delia, D., Kanamaru, A., Kakishita, E., 1995. Establishment and molecular characterization of a novel leukemic cell line with Philadelphia chromosome expressing p230 BCR/ABL fusion protein. Cancer Res. 55 (14), 3192–3196.
Walensky, L.D., Kung, A.L., Escher, I., et al., 2004. Activation of apoptosis in vivo by a hydrocarbon-stapled BH3 helix. Science 305 (5689), 1466–1470.
Wang, J., Pendergast, A.M., 2015. The emerging role of ABL kinases in solid tumors. Trends Cancer 1 (2), 110–123.
Weisberg, E., Manley, P., Mestan, J., Cowan-Jacob, S., Ray, A., Griffin, J.D., 2006. AMN107 (nilotinib): a novel and selective inhibitor of BCR-ABL. Br. J. Cancer 94 (12), 1765–1769.
Weisberg, E., Manley, P., Mestan, J., Cowan-Jacob, S., Ray, A., Griffin, J.D., 2019. Correction: AMN107 (nilotinib): a novel and selective inhibitor of BCR-ABL. Br. J. Cancer 121 (3), 282. -282.
Wishart, D.S., Knox, C., Guo, A.C., Shrivastava, S., Hassanali, M., Stothard, P., Chang, Z., Woolsey, J., 2006, Jan 1. DrugBank: a comprehensive resource for in silico drug discovery and exploration. Nucleic Acids Res. 34 (Database issue), D668–D672.
Wojtowicz, W., Wróbel, A., Pyziak, K., Tarkowski, R., Balcerzak, A., Bębenek, M., Młynarz, P., 2020. Evaluation of MDA-MB-468 cell culture media analysis in predicting triple-negative breast cancer patient sera metabolic profiles. Metabolites 10 (5), 173.
Yelskaya, Z., Carrillo, V., Dubisz, E., Gulzar, H., Morgan, D., Mahajan, S.S., 2013. Synergistic inhibition of survival, proliferation, and migration of U87 cells with a combination of LY341495 and Iressa. PLoS One 8 (5), e64588.
Zhang, J., Liu, J., Wang, Y., Zhang, B., 2016. Novel therapeutic strategies for patients with triple-negative breast cancer. Onco Targets Ther. 9, 6519–6528.
Zheng, L., Wang, Y., Sheng, J., et al., 2011. Antitumor peptides from marine organisms. Mar. Drugs 9, 1840–1859.
Zhong, L., Li, Y., Xiong, L., Wang, W., Wu, M., Yuan, T., Yang, W., Tian, Ch., Miao, Z., Wang, T., Yang, S., 2021. Small molecules in targeted cancer therapy: advances, challenges, and future perspectives. Sig. Transduct. Target Ther. 6 (1), 1–48.
Zhou, T., Commodore, L., Huang, W.S., Wang, Y., Thomas, M., Keats, J., Hu, Q., Rivera, V.M., Shakespeare, W.C., Clackson, T., Zhu, X., 2011. Structural mechanism of the pan-BCR-ABL inhibitor ponatinib (AP24534): lessons for overcoming kinase inhibitor resistance. Chem. Biol. Drug Des. 77, 1–11.